# Analysis of P-wave travel times for teleseismic earthquakes on nodal seismic surveys

**Steve Hearn**
*Velseis Pty Ltd and University of Queensland*
steveh@velseis.com

**Bodee Bignell**
*University of Queensland*
bodee.bignell@uq.net.au

**John Mc Monagle**
*Velseis Pty Ltd*
johnmc@velseis.com

**Shaun Strong**
*Velseis Pty Ltd*
sstrong@velseis.com

**SUMMARY**

Nodal seismic systems record continuously, and hence record a range of passive events. With severe high-cut filtering it is possible to extract records of teleseismic (distant) earthquakes which are of potential interest in analysis of the crust and upper mantle near the receivers. Cross-correlations of the earthquake P-wave reveal significant inter-nodal time variations, even allowing for near surface static effects. These variations may relate to geology within the sedimentary section, and deeper in the crust.

Because of the large channel counts in modern surveys, stacking the teleseismic event can provide significant improvement in signal-to-noise. We have used stacked nodal records to infill between recordings made at permanent seismographs in Queensland. Relative travel-time residuals are of order 1-2s. Teleseisms arriving from different azimuths produce conflicting relative-residual patterns. However, ray-path back projection to upper-mantle depths reveals coherent delay patterns. The observations would be consistent with velocity variations of order 10% occurring in the depth zone 200-400km. This supports lateral variation in the degree of development of an upper-mantle low-velocity zone, with low velocities resulting from increased temperature and partial melting.

**Key words**: Nodal system, teleseismic, earthquake, travel-time residual, upper-mantle.

## INTRODUCTION

In the past few years, nodal sensors have emerged as the default for seismic exploration. These systems record continuously, and hence can record a range of passive events in addition to the production events. Nodal systems generally have natural frequencies of 5 Hz or 10 Hz, being designed to record wave frequencies with an upper limit of 100-250 Hz.

On the other hand, waves from teleseismic earthquakes travel thousands of kilometres. They suffer much greater anelastic attenuation and scattering, resulting in dominant frequencies generally less than 1-2 Hz. This is well below the natural-frequency rolloff of the exploration sensor, and hence such events are not readily visible on conventional exploration records. This paper demonstrates that with simple pre-processing it is, however, possible to extract teleseismic P-wave records of surprising quality.

Teleseismic travel-time analysis is highly developed and provides a very simple but powerful tool for investigating seismic velocity variations in the crust and upper mantle. In this paper we illustrate a process for examining time delays between the nodes in a 3D survey. We then investigate the integration of nodal observations with those from regional permanent seismographs.

For these experiments we have examined earthquake P-waves recorded on three different nodal 3D surveys in the Bowen Basin, Queensland. We will refer to these surveys as BB1, BB2, and BB3. Our nodal sensors had a natural frequency of 5 Hz. Six large earthquakes were chosen, occurring during the relevant recording windows. For Survey BB1, epicentral regions and magnitudes were Banda Sea (Mb 7.3), Kermadec (Mb 7.3) and Fiji (Mb 5.8). For Survey BB2, the events were Santa Cruz (Mb 6.6) and Vanuatu (Mb 5.9). For Survey BB3, the event was Kuril Islands (Mb 7.5).

## EXTRACTION of TELESEISMIC P-WAVES

We will illustrate selected aspects of our nodal travel-time analysis with reference to the recording of the large Banda Sea earthquake (Mb 7.3), recorded on approximately 8300 nodes, covering about 4 km2 within the BB1 3D survey. Figure 1 shows a representative single-node record, extracted around the expected arrival time for the earthquake P-wave. For convenience, the continuous record segment is presented as consecutive one minute traces. The uncorrelated sweeps from the production Vibroseis survey dominate the record. The teleseismic event is not obvious.

Figure 2 shows the same recording after application of a severe high-cut filter (attenuation zone 2.5 Hz - 3 Hz). The P-wave train from the Banda Sea event is clearly visible starting at about 37s on Trace 2. Consideration of the earthquake origin time, and the nodal time base provides a P-wave travel time from Banda Sea to Bowen Basin of around 4m 55s, although the event onset is not well defined on individual nodes. Strong surface-wave energy is clearly visible starting about 6-7 minutes after the P-wave.

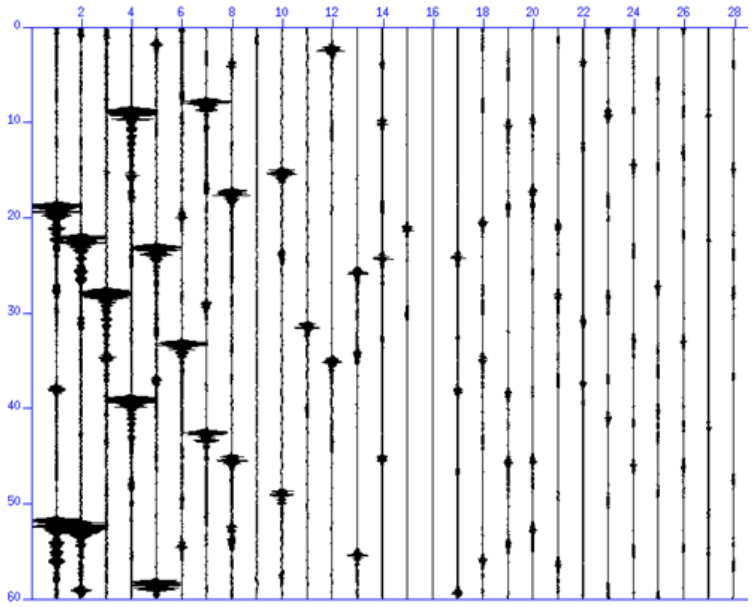


**Figure 1. Representative nodal data segment (BB1 Survey) showing uncorrelated Vibroseis sweeps. Thirty minutes of continuous data are shown, presented as 30 one-minute traces.**

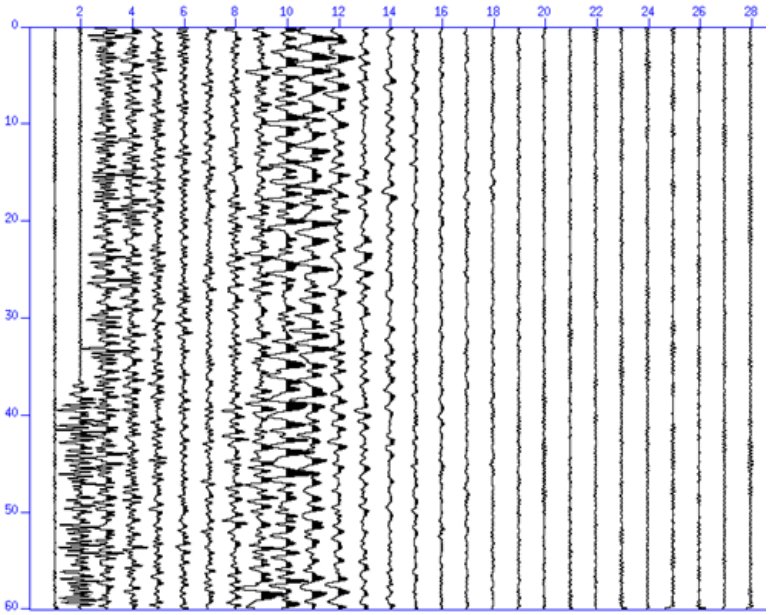


**Figure 2. Representative nodal data segment from Figure 1 after high-cut filtering (2.5 – 3 Hz). The Banda Sea P-wave arrival is at about 37s on Trace 2 (i.e. 97 s after the start of this data segment). Surface wave energy is apparent starting around 6-7 minutes after the P wave.**

## INTER-NODAL TRAVEL-TIME ANALYSIS

For the P-wave travel time analysis we extracted a 10s window for each node, starting just before the apparent P-wave arrival. We obtained relative arrival times across the array by a cross-correlation approach using a 3s window around the P-wave onset. Figure 3 shows the derived relative times for all 8300 nodes, as a function of epicentral distance. The observed slowness (moveout) across the array (~9 s/deg) is consistent with theoretical travel-time models (Event depth: 212 km, Delta: 24 deg).

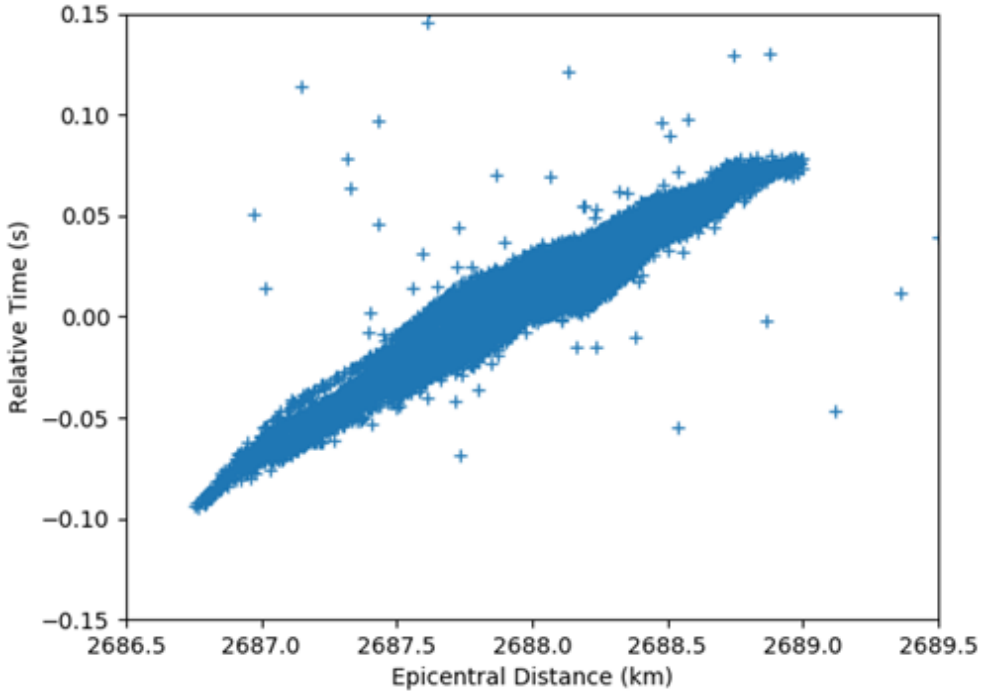


**Figure 3. Relative P-wave travel times for Banda Sea earthquake recorded on 8300 nodes from BB1 survey. In Figures 3 and 4, the zero time corresponds to a travel time of 4m 57.1s, determined via a reference stack trace. Outliers result from failure of the correlation process, and are excluded from the subsequent stacking process.**

Figure 4 shows the same travel-times as in Figure 3, now in map view. The moveout direction across the array is consistent with the azimuth of the Banda Sea event relative to the Bowen Basin site. In Figure 5, the influence of distance has been removed by subtracting theoretical times based on the AK135 Model (Kennett et al., 1995). Other models produce a similar result. This yields a coherent pattern of relative-residuals between array nodes. Nodes towards the NE exhibit significant delays (~ 0.05 s) relative to those in the SW.

One intuitive cause for the residual inter-nodal delays seen in Figure 5 might be surface effects (elevation and weathering variations). To assess this, we examined the receiver static errors derived in the conventional 3D reflection processing. These are shown in Figure 6, plotted with the same colour scale as in Figure 5. Clearly, the observed inter-nodal variations in Figure 5 are much too large to be explained by the near surface changes in Figure 6. Figure 7 emphasises this, showing the difference between these figures, i.e. the relative residuals with the surficial statics removed. The final range of inter-nodal relative residuals is around 0.04 s. If real, these delays most likely originate within the sedimentary section, or deeper in the crust.

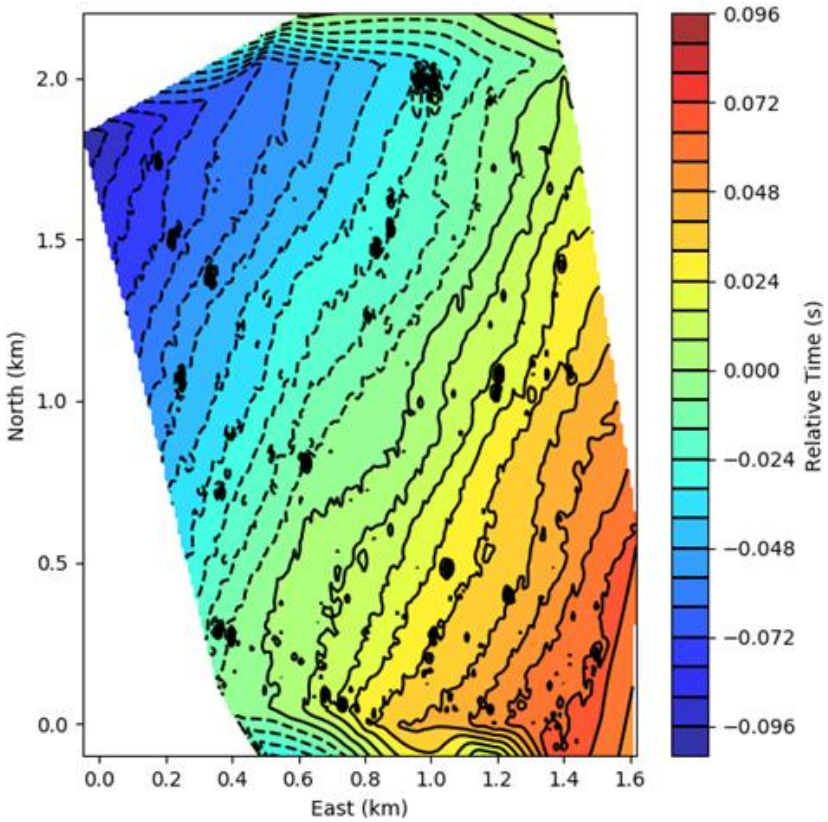


**Figure 4. Relative P-wave travel times for the Banda Sea earthquake (Figure 3) presented in map view. The epicentre is towards the NW. Anomalies at top and bottom are contouring edge effects. The range of times is about 0.2s.**

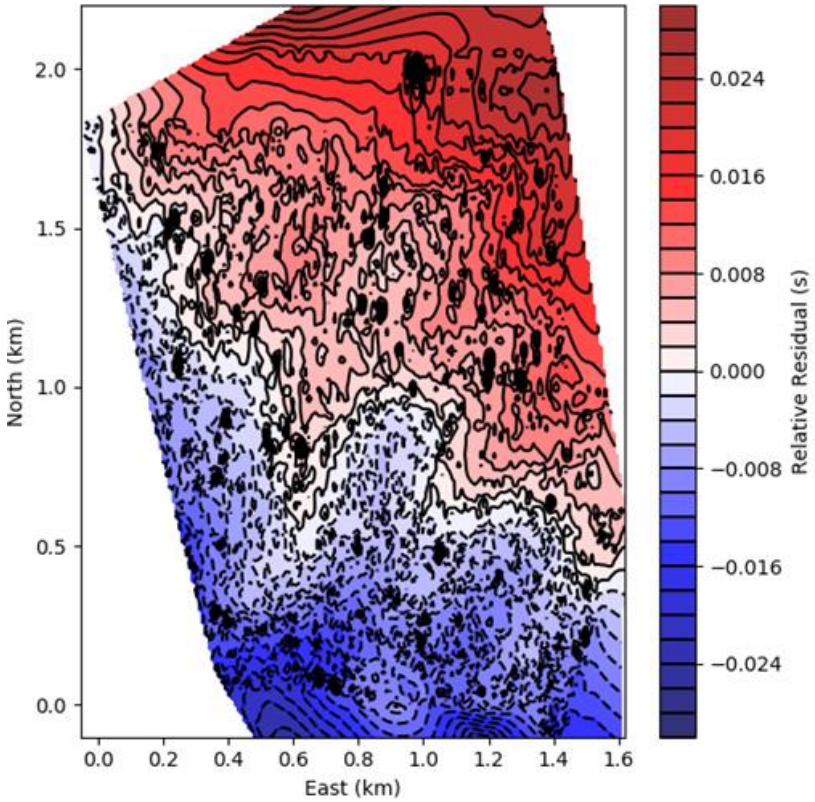


**Figure 5. Relative P-wave residuals between nodes in the BB1 survey, following removal of distance effects from data in Figure 4, using the AK135 model. The distance correction reduces the range of times from 0.2 s to 0.05 s.**

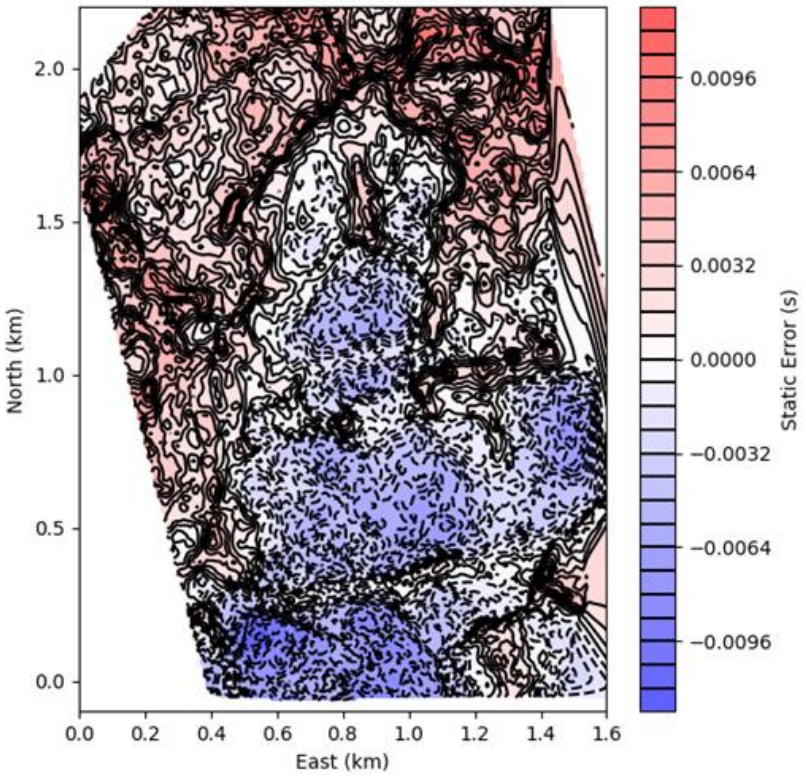


**Figure 6. P-wave receiver static errors derived from 3D reflection processing. This represents the effects of elevation and weathering variations. The colour scale is the same as in Figure 5.**

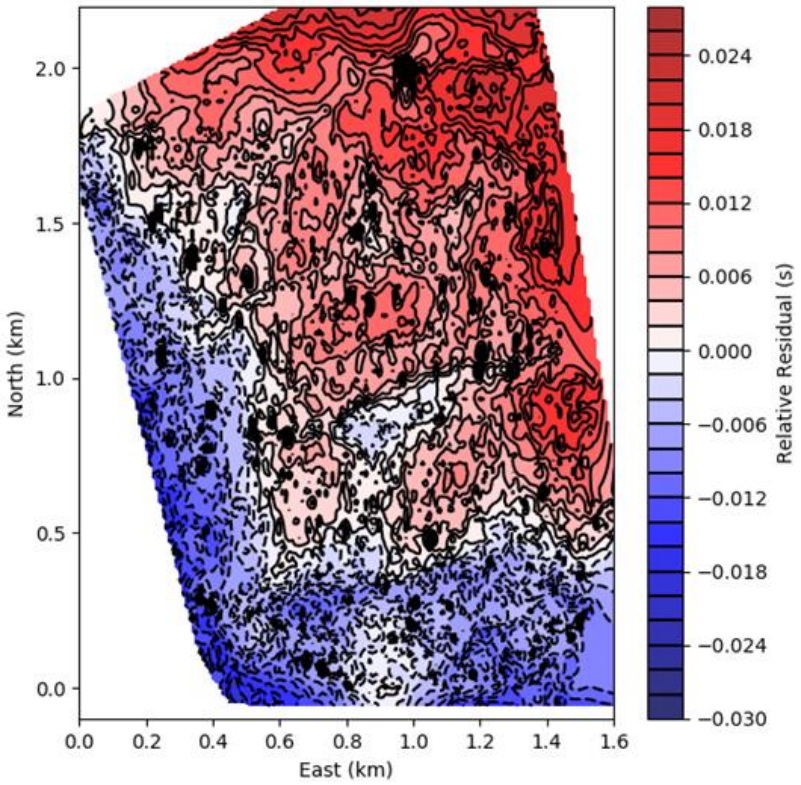


**Figure 7. Inter-nodal residuals (Figure 5) following subtraction of surficial statics (Figure 6). The colour scale is the same as in Figures 5 and 6.**

## INTEGRATION WITH PERMANENT SEISMOGRAPHS

It is of interest to compare the overall delay for the BB1 survey with delays seen at other permanent seismographs in the region. For this purpose we need to define an absolute arrival time for the composite BB1 array. Accurate determination of the precise onset is difficult on individual nodes, and there is considerable variability between nodes (Figure 8, top).

Because of the high channel count (8300), stacking provides a significant improvement in signal-to-noise ratio. The stacked trace (Figure 8, bottom) is much more stable prior to the P-wave onset and allows improved estimation of the arrival time, apparently to an accuracy of about 0.1s. This appears adequate for integration with data from permanent seismographs, as confirmed below.

The stacking process is of interest. In Figure 8 (bottom) the orange trace represents the stack obtained by aligning all 8300 traces perfectly in time prior to the stack. That is, all distance effects, and inter-nodal residuals (Figure 5) are removed prior to stacking. The blue trace is obtained with a raw stack with no time corrections. Alignment does slightly improve the amplitudes in later (higher-frequency) arrivals. However, alignment provides no improvement to the P-wave onset, due to its low-frequency character.

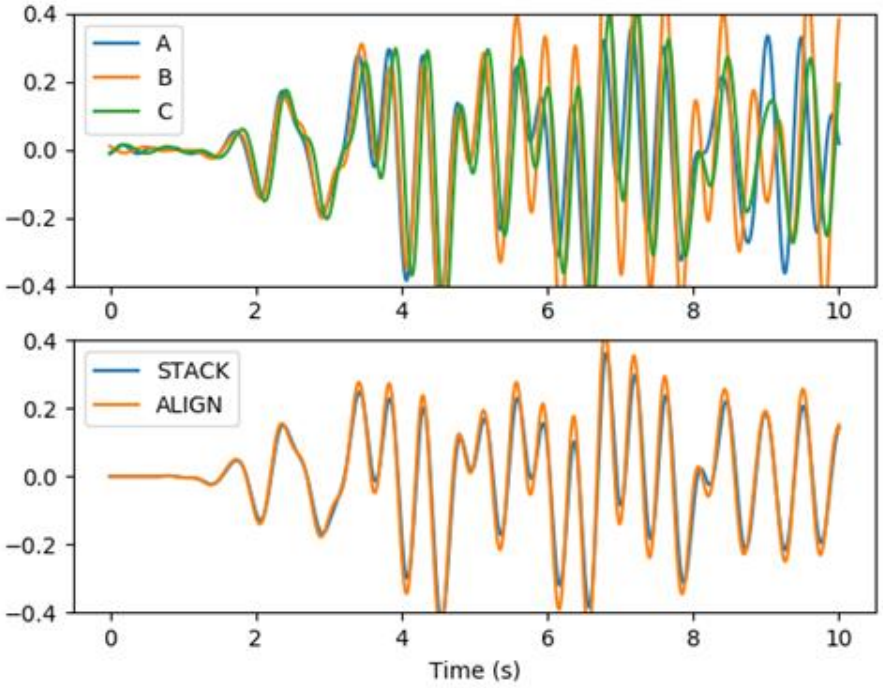


**Figure 8. (Top) Representative nodal recordings of the Banda Sea event, for three nodes selected at random across the survey. The P-wave onset is expected to be a negative break. (Bottom) Stacks of all 8300 traces derived using no alignment (blue) and time alignment (orange). The negative-break is at about 1.1s**

Figure 9 compares the stacked BB1 trace with recordings from twelve permanent seismographs in Queensland and northern New South Wales. Traces are time shifted with epicentral distance, such that the expected AK135 arrival time is zero. Clearly there are relative time residuals in excess of 1.5 s. The different instrument response of the nodal site BB1 is obvious.

Figure 10 presents the relative time residuals measured from Figure 9 in map view, following elevation correction. Despite the different system response of the nodal trace, the picked time appears geographically consistent with the surrounding stations. Figure 11 shows a similar geographical plot for relative residuals from the Kermadec event, which is at roughly the opposite azimuth to the Banda Sea event.

The relative-residual patterns for the two events at different azimuths are strikingly different. This is not unusual in relative residual analysis (e.g. Bolt and Nuttli, 1966; Hearn and Webb, 1984; Engdahl and Ritzwoller, 2001). The station residuals in Figures 10 and 11 have been plotted at the surface coordinates of the stations. The inconsistency observed between the two figures implies that the causative velocity anomalies cannot occur close to the surface.

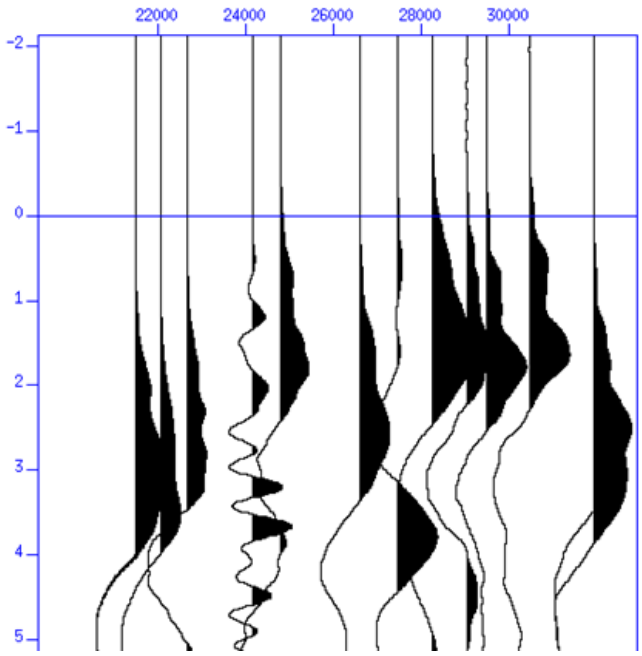


**Figure 9. Comparison of BB1 stack trace (Trace 4) with recordings from permanent seismographs for Banda Sea event. Station codes are included in Figure 10. The first break is positive on all traces. (The BB1 trace has been polarity reversed, to accommodate the different conventions on seismometers and geophones).**

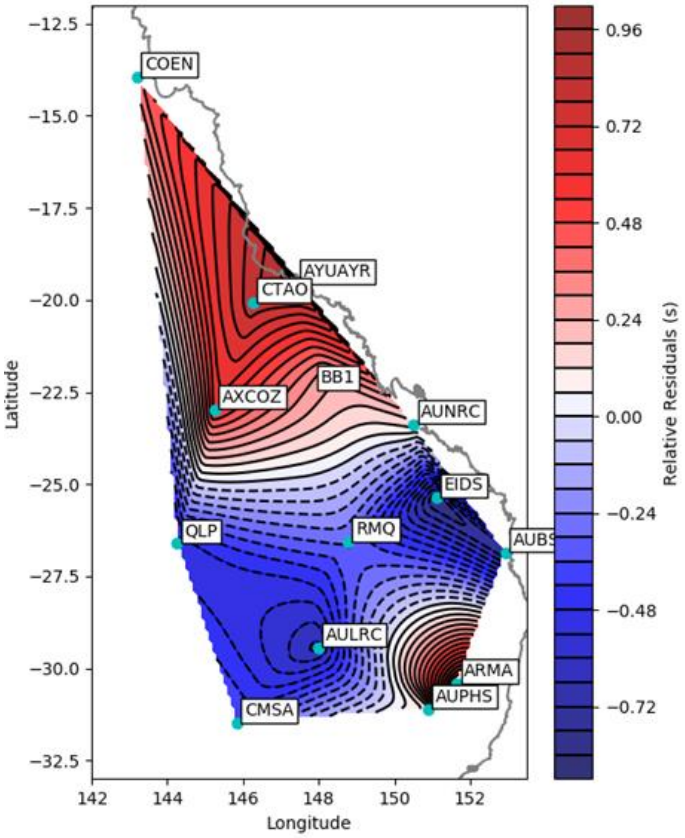


**Figure 10. Relative residuals for Banda Sea event, plotted relative to the mid-range value. Blue and red correspond to early and late arrivals. Codes and locations of permanent stations, and the general location of nodal station BB1, are shown.**

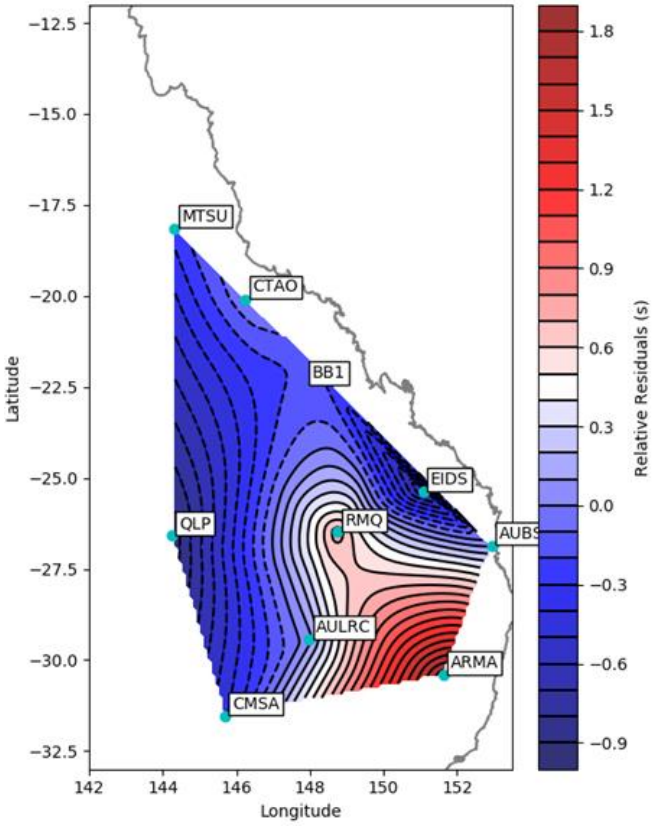


**Figure 11. Relative residuals for Kermadec event, at approximately opposite azimuth to the Banda Sea event. Residuals are plotted relative to the mid-range value. Compare with Figure 10.**

A simple approach to investigating this inconsistency is to project residual observations below the surface, by raytracing from each station back towards the epicentre. The hypothesis is that consistency should improve as the residuals are projected closer to causative anomalies. Figure 12 illustrates the general concept. In addition to the two earthquakes discussed above, three additional events are included, to provide more azimuthal control. In Figure 12 (left), residuals have been projected back along raypaths to a depth of 50 km. Clearly there are still significant inconsistencies. The contouring algorithm forces very high gradients near some stations, in an attempt to satisfy conflicting observations. Figure 12 (right) shows a projection to 250km depth. Now the contour pattern is much simpler, with most inconsistencies resolved. We find that the region to the NE simplifies further in a projection to 350 km. Our full depth analysis suggests that the causative anomalies for these regional relative residuals are most likely in the upper mantle, predominantly in the depth zone 200-400 km.

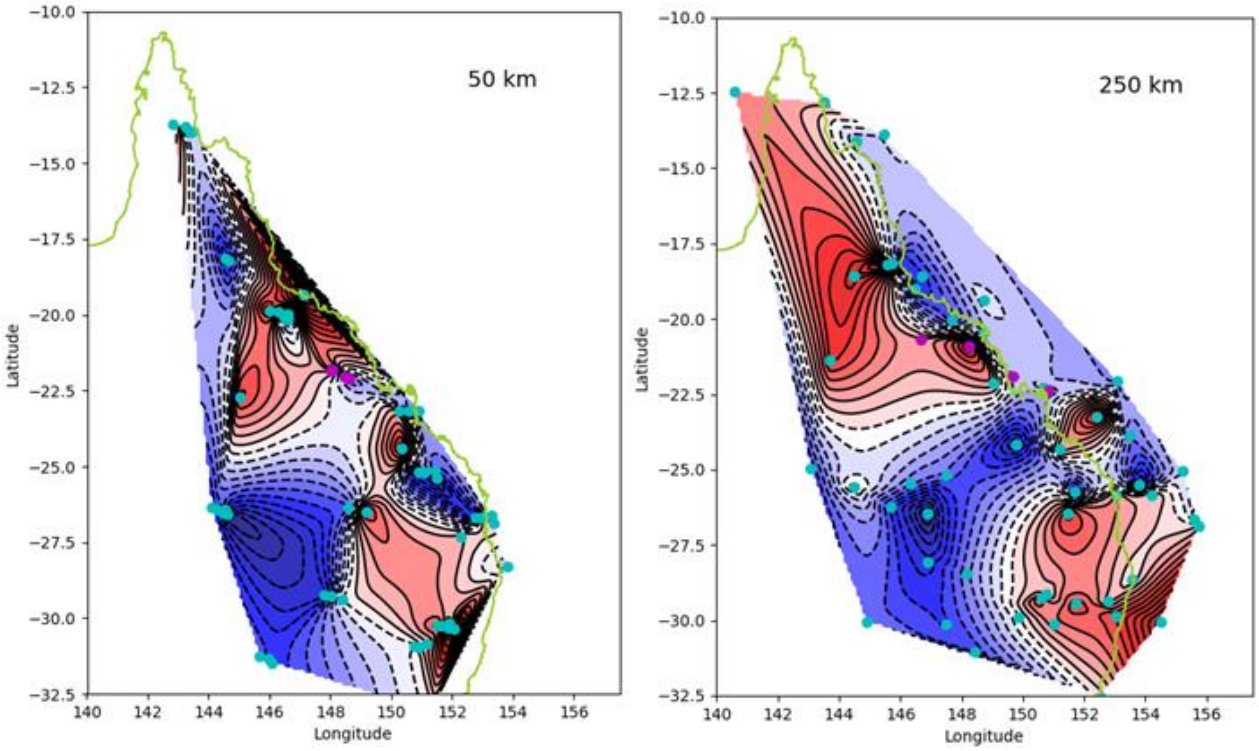


**Figure 12. Examples of back projection of relative residuals for five earthquakes at multiple azimuths (Banda Sea, Kermadec, Fiji, Vanuatu, Kuril) recorded at permanent (blue) and nodal (purple) surveys. Range of relative residuals: -1s (blue, early) to +1s (red, late). LEFT, back-projection to depth=50 km. RIGHT, back-projection to depth=250 km.**

## CONCLUSIONS

Because nodal seismic systems record continuously they have potential for recording non-survey events. Teleseismic earthquake arrivals have dominant frequencies below the natural sensor frequency and are not visible on production records. However with appropriate filtering, viable records emerge. Significant travel-time variations can be detected between nodes in a survey. These cannot be explained by distance effects, or by surficial static errors. The intuitive geological explanation relates to variations within the sedimentary section, or deeper crust.

Typical 3D nodal surveys use thousands of receivers. The survey can be thought of as an array for larger scale studies. Signal-to-Noise is improved significantly on the stacked trace, making the teleseismic P-wave onset easier to pick. Although the nodal array has quite different response, the picked arrival times from the nodal arrays integrate smoothly into residual patterns obtained from regional permanent seismographs.

An analysis of regional relative residuals has been improved by the inclusion of nodal data, and is broadly consistent with an earlier study (Hearn and Webb, 1984). The observed residuals are consistent with variations in upper-mantle velocities in the depth zone 200-400 km. The observed relative residuals (~ 1.5s) imply velocity variations of order 10% extending over depth zones of order 100km. This may relate to differential development of an upper-mantle low-velocity zone.

**ACKNOWLEDGMENTS**

We acknowledge the anonymous client companies whose nodal surveys prompted this study. Permanent seismograph data were obtained from the IRIS Data Services Wilber 3 system.

**REFERENCES**

Bolt, B.A., and Nuttli, O.W., 1966, P wave residuals as a function of azimuth: 1. Observations: Journal of Geophysical Research, 71, 5977-5985.

Engdahl, E.R. and Ritzwoller, M.H., 2001, Crust and upper mantle P- and S-wave delay times at Eurasian seismic stations: Physics of the Earth and Planetary Interiors, 123, 205-219.

Hearn S.J, and Webb, J.P., 1984, Relative teleseismic P residuals and upper-mantle structure in Eastern Queensland, Australia: Bulletin Seismological Society America,74, 1661-1681.

Kennett, B.L.N. Engdahl, E.R. and Buland R., 1995. Constraints on seismic velocities in the Earth from travel times, Geophysical Journal International, 122, 108-124.